Doppler Effect Mitigation over Mobile Underwater Acoustic OFDM System

Jingxin Xu[1], Deqing Wang[*,1,2], Xiaoyi Hu[1], Yongjun Xie[1]
1. Key Laboratory of Underwater Acoustic Communication and Marine Information Technology (Xiamen University), Ministry of Education, Xiamen, Fujian, China
2. Key Laboratory of Technology and Application For Safeguarding of Marine Rights and Interests, SOA, Guangzhou, Guangdong, China
23320161153441@stu.xmu.edu.cn, {deqing, xyhu, xyj}@xmu.edu.cn

ABSTRACT

Orthogonal frequency division multiplexing (OFDM) has prevailed in high speed underwater acoustic(UWA) communications with obvious multipath effects. However, with the characteristic of being sensitive to the Doppler effect, the performance of an OFDM system is severely limited by the intercarrier interference (*ICI*) introduced by Doppler spread. In this paper, we build a hydroacoustic baseband defferentially encoded OFDM system and propose an effective approach to mitigate the Doppler effect for the system. After utilizing the Chirp-Z transform(*CZT*) to estimate a coarse common value of large scale Doppler factor a and null subcarriers for the estimation of residual Doppler a_m for each OFDM symbol, we use the method of polyphase filter resampling to compensate them. We also correct the phase rotation effect caused by timing sampling offset according to the residual Doppler estimation result. Simulation and experimental results show that while meeting the accuracy requirement of Doppler scaling factor estimation in mobile UWA communications, the proposed algorithm can be used to accurately and effectively estimate the Doppler scaling factor and requires lower computational complexity.

CCS CONCEPTS

• **Underwater communications**; • **Underwater experimentation and deployments**;

KEYWORDS

Mobile underwater acoustic communication, OFDM, Doppler scaling factor, estimation and compensation

∗ The corresponding author.

WUWNet'18, December 3–5, 2018, Shenzhen, China

ACM ISBN 978-1-4503-6193-4/18/12…$15.00
https://doi.org/10.1145/3291940.3291965

1 INTRODUCTION

Compared with the traditional single-carrier communication system, OFDM has the advantages of anti-multipath, high spectral efficiency and implementing simply. In recent years, OFDM communication systems have been one of the main solutions for high-rate UWA communications[15]. However, it is susceptible to Doppler shift. Especially in the UWA communications with relatively low speed of sound($\approx 1500 m/s$), the relative movement between communication carriers, the asynchronization between carriers caused by the deviation of crystal oscillations in the receiving and transmitting systems, the reflections of moving objects(waves, etc.) and other phenomena lead to large Doppler shift[6][12],[16]. It brings *ICI* and severely restricts the performance of OFDM in mobile acoustic communication.

At present, researches on Doppler scaling factor estimation for mobile UWA communications can be summarized as the time-domain method and frequency-domain one. The former is based on the end-to-end synchronization signal or the self-cyclic shift sequence. And the latter is aimed to measuring frequency offset based on probing signals. Reference [14] and [18] involve transmitting Doppler-insensitive preamble and postamble at the beginning and end of each frame of signal to estimate the overall Doppler scaling factor. However, the use of preamble and postamble makes the estimation only possible after the signal transmission is completed, which leads to the losing of characteristic of real-time processing. In addition, reference [7] relies on single-frequency signal as a training sequence to estimate the Doppler frequency offset roughly, and then relies on *FFT* to compensate the Doppler frequency offset. Furthermore, another method is that a Doppler-sensitive waveform like Costa waveform[2],m-sequence and poly-phase sequence[3] is transmitted as a preamble. At the receiver, a bank of correlators correlates the received signal with preambles prescaled by different Doppler scaling factors, and the branch with the largest correlation peak provides the estimated Doppler scale.In all schemes above, Doppler spreads of OFDM symbols are only compensated according to the overall estimated value for a data package. While with fast-varying movements, the Doppler estimation and compensation should also be performed with every received data symbol[8].

On the basis of reference[14], a method of setting null subcarriers is proposed in reference[5]. It can search for the residual Doppler factor by using multiple signal classification(*MUSIC*) algorithm to minimize the cost function(total energy on null subcarriers). The

method can track the time-varying Doppler for each OFDM sysmbol. But many times of resampling and *FFT* according to the tentative Doppler shifts in estimation range lead to a large amount of computation, which is not conducive for real-time communication.

A variety of non-time domain algorithms have also been successfully applied to UWA communication, such as frequency measurement based on *ZOOM-FFT*, Interpolation *FFT*[17], correlation peak searching based on thumb-tack ambiguity function, etc. However, some of these frequency-domain estimation methods like *ZOOM-FFT* and Interpolation *FFT* limited to estimation accuracy of f_s/N can not meet the requirement. And the others like complexes correlation require multiple iterations to obtain the estimation value. They need much amount of computation and are not suitable for the real-time tracking of Doppler scaling factor.

To solve the contradiction between estimation accuracy and amount of computation(real-time), in this paper, we have established a baseband differentially encoded OFDM system[4] and propose a method for estimating Doppler in Chapter 2. As for the proposed estimation method, it can track the real-time Doppler factor for each OFDM symbol and take into account the computational complexity and accuracy of estimation and compensation. Based on the existing *wideband to narrowband* Doppler estimation method[5], because the frequency offsets on different subcarriers of an OFDM symbol are non-uniform(depend on the frequency of subcarriers), we here convert the frequency offset problem to the problem of Doppler scaling factor solution:$a = \Delta f/f_c$ and have a higher estimation accuracy.

When estimating Doppler, we firstly use Chirp-Z transform(*CZT*)[13] to coarsely estimate the overall Doppler scaling factor a. It will narrow the estimation range for the subsequent residual Doppler estimation. Compared to *FFT*-based frequency measurement, it minimizes the spectral leakage and improve the estimation accuracy. And then, residual Doppler estimation relying on null subcarriers can separately obtain the residual Doppler factor corresponding to each OFDM symbol. For reducing the amount of calculation, we replace the original method of estimation range traversal[5] by the method of estimation range dichotomy. It can achieve the effect of real-time tracking and estimation.

To compensate Doppler, Large-scale Doppler compensation and residual Doppler compensation are conducted by means of polyphase filter resampling. In addition, according to the required deviation points gotten by the described residual Doppler estimation, we further mitigate different phase rotation effects due to the sampling timing offset[9] on each subcarrier of each symbol. It will further reduce the error rate at the receiver and improve the system performance.

2 SYSTEM MODEL

In this paper, we construct the proposed algorithm of Doppler estimation and compensation for mobile underwater acoustic OFDM communication in a baseband OFDM time-domain differential(TD) system. Fig.1 is the framework of the baseband OFDM system. Compared to the passband OFDM system[4], the baseband one does not need the upper frequency modulation at the transmitter and the lower frequency demodulation at the receiver. The data is modulated on the subcarriers in the corresponding frequency band as

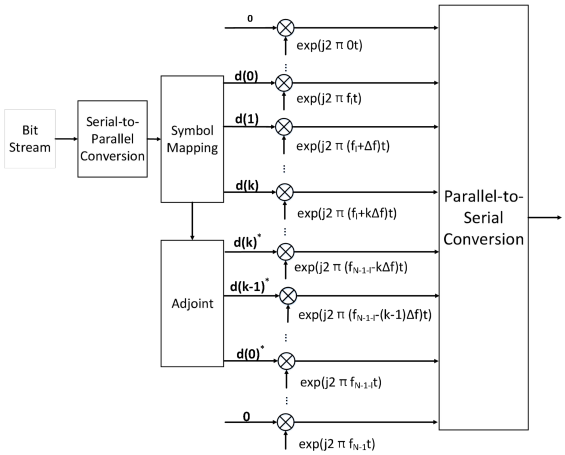

Figure 1: Framework of the baseband OFDM transmitter.

$f_l \sim f_l + k\Delta f$ shown in Fig.1. The placement of conjugate data on symmetric subcarriers makes the output of *IFFT* modulation is real data, which makes it unnecessary to process the separate real and imaginary parts of the data and further simplifies the transmitter structure compared to the bandpass system. We regard that the phase effect of the channel on two adjacent OFDM symbols is similar. So using the phase differential modulation and demodulation, we can eliminate QPSK signal phase rotation caused by channel transmission at the receiver. And therefore we don't need channel estimation, which raises the information transmission rate and avoids the system performance degradation due to inaccuration of channel estimation.

The block diagram of our system is shown in Fig.2. After serial-to-parallel conversion, 4DPSK (Differential Phase Shift Keying) and null subcarriers insertion (for residual Doppler estimation), the source bitstream in the transmitter undergoes OFDM modulation and serial-to-parallel conversion. Subsequently, we insert probing and chirp signal into transmitted signal for large-scale Doppler estimation and signal synchronization at the receiver. The probing signal consists of three single-frequency sequences $s_1(t), s_2(t), s_3(t)$ with frequencies f_1, f_2, f_3, respectively. As is shown in Fig.3, a single-frequency probing signal of two transmission modes of serial and parallel is inserted into the transmission frame format. In the following, we compare the Doppler estimation accuracy of the two modes. In the implementation, depending on the system requirements, designers can choose one of serial mode or parallel mode.

For the purpose of signal timing synchronization, we use chirp with obvious correlation peak to ascertain the starting position of the received OFDM signal. As is shown in Fig.2, the proposed Doppler estimation and compensation algorithm consists of two steps: I large-scale Doppler estimation and compensation, II residual Doppler estimation and compensation.

About the 4DPSK modulation of system framework shown in Fig.2, let $d_{m-1}[k]$ denote the DQPSK(Differential QPSK) symbol on the k-th subcarrier of the $m-1$-th OFDM symbol. The DQPSK symbol on the k-th subcarrier of the m-th OFDM symbol is then given by

$$d_m[k] = mod(d'_m[k] + d_{m-1}[k], 4), \tag{1}$$

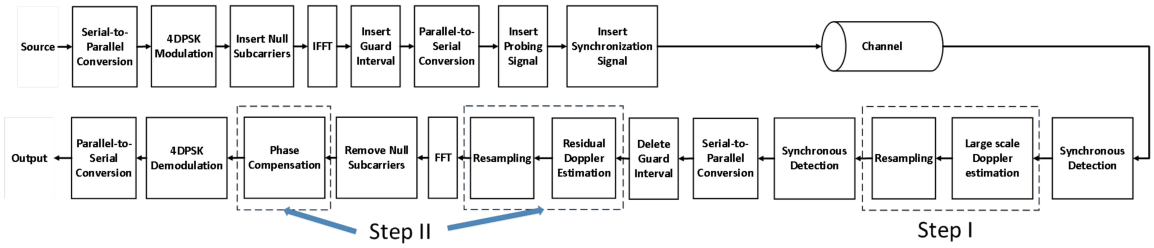

Figure 2: Framework of the proposed Doppler estimation and compensation algorithm.

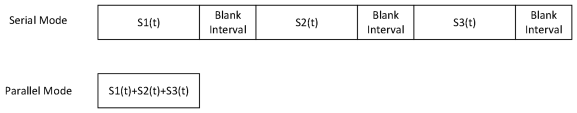

Figure 3: Block structure of the implemented OFDM-based UWA system using the proposed algorithm

where $d'_m[k]$ denotes the QPSK symbol on the k-th subcarrier of the m-th OFDM symbol.

As for OFDM modulation, we assume that the m-th OFDM symbol to be transmitted is

$$s_m(t) = \sum_{k=0}^{N-1} d_m[k] e^{j2\pi f_k t} g(t), \tag{2}$$

where

$$g(t) = \begin{cases} 1 & t \in [0, T + T_{cp}] \\ 0 & \text{otherwise} \end{cases},$$

and T denotes the OFDM symbol duration and T_{cp} cyclic prefix. $f_k = k/T$ is the frequency of the k-th subcarrier and $d_m[k]$ is the DQPSK symbol corresponding to the k-th subcarrier of the m-th OFDM symbol. Then we consider a multipath underwater channel whose impulse response for the m-th OFDM symbol is

$$c_m(\tau; t) = \sum_{l=1}^{L} A_l(t)\delta(\tau - \tau_l(t)), \tag{3}$$

where $A_l(t)$ is the path amplitude and $\tau_p(t)$ is the time-varying path delay. We treat $A_l(t)$ to be A_l (constant) during an OFDM symbol and suppose the channel as having a common Doppler scaling factor on all propagation paths but different ones for different OFDM symbols. So the delay variation can be approximated by a first-order polynomial of its Taylor expansion:

$$\tau_l(t) \approx \tau_l - (a + a_m)t, \tag{4}$$

where a is the common large scaling factor and a_m is the residual one for m-th OFDM symbol. So the channel impulse response can be approximated as

$$c_m(\tau; t) = \sum_{l=1}^{L} A_l \delta(\tau - \tau_l + (a + a_m)t). \tag{5}$$

Assume that the synchronization is accurate, we can remove the cyclic prefix, and the received m-th OFDM symbol is

$$\begin{aligned} r_m(t) &= \sum_{k=0}^{N-1} d_m[k] \sum_{l=1}^{L} A_l e^{j2\pi f_k (t - \tau_l + (a+a_m)t)} \\ &\quad \cdot g(t - \tau_l + (a + a_m)t) + n(t) \\ &= \sum_{k=0}^{N-1} d_m[k] e^{j2\pi f_k ((1+a+a_m)t)} \\ &\quad \cdot \sum_{l=1}^{L} A_l e^{-j2\pi f_k \tau_l} g(t - \tau_l + (a + a_m)t) + n(t), \end{aligned} \tag{6}$$

where $n(t)$ is the additive noise. After large scale Doppler estimation, we get the estimation value of common large scale Doppler factor a: $\hat{a}$. We resample the signal with $\hat{a}$:$y_m(t) = r_m(\frac{t}{1+\hat{a}})$, and obtain Eq.7:

$$\begin{aligned} y_m(t) &= \sum_{k=0}^{N-1} d_m[k] e^{j2\pi f_k t} e^{j2\pi f_k \frac{(a-\hat{a}+a_m)}{1+\hat{a}} t} \\ &\quad \cdot \sum_{l=1}^{L} A_l e^{-j2\pi f_k \tau_l} g(\frac{1 + a + a_m}{1 + \hat{a}} t - \tau_l) + n'(t), \end{aligned} \tag{7}$$

$n'(t)$ is the additive noise after resampling. For the sake of theoretical derivation, we omit the gate function $g(t)$ and the m-th symbol interference term due to multipath $\sum_{l=1}^{L} A_l e^{-j2\pi f_k \tau_l}$ is defined as H_k^m, then Eq.7 is modified as

$$y_m(t) = \sum_{k=0}^{N-1} d_m[k] \cdot H_k^m e^{j2\pi f_k t} e^{j2\pi f_k \frac{a-\hat{a}+a_m}{1+\hat{a}} t} + n'(t). \tag{8}$$

To further refine the residual Doppler $\frac{a-\hat{a}+a_m}{1+\hat{a}}$ for each OFDM symbol, we define it as β_m and its estimated value as $\hat{\beta}_m$ for convenience. If $\hat{\beta}_m = \beta_m$, after resampling according to $\hat{\beta}_m$:$z_m(t) = y_m(\frac{t}{1+\hat{\beta}_m})$, we can obtain Eq.9:

$$\begin{aligned} z_m(t) &= \sum_{k=0}^{N-1} d_m[k] \cdot H_k^m e^{j2\pi f_k \frac{1-\beta}{1+\beta} t} + n''(t) \\ &= \sum_{k=0}^{N-1} d_m[k] \cdot H_k^m e^{j2\pi f_k t} + n''(t). \end{aligned} \tag{9}$$

If we do the discretization of received signal with sampling interval T_s and sampling length N, then the duration of the m-th symbol is $[T_{cp} + \Delta t_m, T_{cp} + T + \Delta t_m]$. Here T_{cp} and T denote cyclic prefix

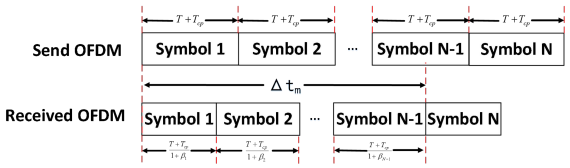

Figure 4: Sampling timing offset due to residual Doppler

length and OFDM symbol length without cyclic prefix,respectively. As is shown if Fig.4, Δt_m is the sampling timing offset accumulated due to the existence of the residual Doppler factor for the m-th symbol:

$$\Delta t_m = \begin{cases} 0 & m = 1 \\ \sum_{i=1}^{m-1} (T + T_{cp}) \frac{1}{1+\beta_i} & m > 1 \end{cases}. \tag{10}$$

And we know $f_k = \frac{k}{NT_s}, T_{cp} = N_{cp}T_s, T = NT_s, \Delta t_m = \Delta N_m T_s$. For convenience, after omitting the noise and sampling, the signal can be denoted as

$$\begin{aligned} Z_m[n] &= z_m(nT_s + T_{cp} + \Delta t_m) \\ &= \sum_{k=0}^{N-1} \{d_m[k] \cdot H_k^m e^{j2\pi k(n+N_{cp}+\Delta N_m)/N}\} \\ &= \sum_{k=0}^{N-1} \{d_m[k] \cdot H_k^m e^{j2\pi kn/N} \cdot e^{j2\pi k\Delta N_m/N} \cdot e^{j2\pi kN_{cp}/N}\}. \end{aligned} \tag{11}$$

After FFT demodulation $\tilde{d}_m[p] = \sum_{n=0}^{N-1} Z_m[n] e^{-j2\pi pn/N}$, the data on the p-th subcarrier can be denoted as

$$\begin{aligned} \tilde{d}_m[p] &= \sum_{k=0}^{N-1} \{d_m[k] H_k^m \cdot \sum_{n=0}^{N-1} e^{j2\pi \frac{k-p}{N} n} \cdot e^{j2\pi \frac{k}{N} N_{cp}} \cdot e^{j2\pi \frac{k}{N} \Delta N_m}\} \\ &= d_m[p] \cdot H_p^m \cdot N \cdot \varphi_m[p] \cdot \phi_m[p,p] \\ &+ \sum_{k=0, k\neq p}^{N-1} d_m[k] \cdot H_k^m \cdot \varphi_m[k] \cdot \phi_m[p,k] \\ &= d_m[p] \cdot H_p^m \cdot N \cdot \varphi_m[p] \cdot \phi_m[p,p] + \zeta_m[p], \end{aligned} \tag{12}$$

where

$$\varphi_m[p] = e^{j2\pi \frac{p}{N} N_{cp}},$$

$$\phi_m[p,p] = e^{j2\pi \frac{p}{N} \Delta N_m},$$

$$\phi_m[p,k] = e^{j2\pi \frac{k}{N} \Delta N_m}, k \neq p,$$

$\varphi_m[p]$ is the phase rotation on the p-th subcarrier of the m-th symbol due to removing the cyclic prefix. This term is a constant after the difference between symbols for non-coherent OFDM systems. $\phi_m[p,k]$ can be regarded as the additive interference of the k-th subcarrier of the m-th symbol to the p-th subcarrier. We treat it as noise in this paper and do not process it. $\phi_m[p,p]$ can be seen as the sampling timing offset due to the appearance of the residual Doppler factor, causing phase rotation on the p-th subcarrier.

So after compensating the phase rotation due to the sampling timing offset and omitting the noise term $\zeta_m[p]$, the demodulated symbol can be denoted as

$$\begin{aligned} \hat{d}_m[p] &= \tilde{d}_m[p] \cdot e^{-j2\pi \frac{p}{N} \Delta N_m} \\ &\approx d_m[p] \cdot H_p^m \cdot e^{j2\pi \frac{p}{N} N_{cp}}. \end{aligned} \tag{13}$$

Because we use differential demodulation, the transfer function H_p^m due to multipath between adjacent symbols is considered not to change too much that $H_p^m \approx H_p^{m-1}$:

$$\begin{aligned} d'_m[p] &= \frac{\hat{d}_m[p]}{\hat{d}_{m-1}[p]} \\ &= \frac{d_m[p] \cdot H_p^m \cdot e^{j2\pi \frac{p}{N} N_{cp}}}{d_{m-1}[p] \cdot H_p^{m-1} \cdot e^{j2\pi \frac{p}{N} N_{cp}}} \\ &= \frac{d_m[p]}{d_{m-1}[p]}. \end{aligned} \tag{14}$$

3 PRINCIPLE OF DOPPLER ESTIMATION AND COMPENSATION ALGORITHM

In this paper, we propose a *two-step* approach to mitigating the Doppler effect due to fast time-varying UWA channels: I large scale Doppler estimation and compensation, II residual Doppler estimation and compensation. The following is a detailed description of the *two-step* scheme of Doppler estimation and compensation proposed in this paper.

3.1 Large scale Doppler Estimation and Compensation

According to the single-frequency sequences with frequencies f_1, f_2, f_3 respectively, we can get a coarse estimated Doppler factor by using CZT. Assume that the received sequence is $y(n)$, then its CZT result can be expressed as

$$Y[z_k] = \sum_{n=0}^{M-1} y[n] A^{-n} W^{kn}, 0 \leq k \leq M-1, \tag{15}$$

where $A = e^{j\theta_0}$,$W = e^{-jh_0}$. By setting θ_0 and h_0, the initial frequency and the frequency interval can be set correspondingly so that the estimation accuracy is adjusted. Here we make them as

$$\theta_0 = 2\pi \frac{f_n(1 - a_{max})}{f_s}, 1 \leq n \leq 3, \tag{16}$$

$$h_0 = \frac{2\pi f_n \times 2a_{max}}{Mf_s}, 1 \leq n \leq 3, \tag{17}$$

a_{max} is the maximum Doppler scaling factor set based on empirical value in actual mobile UWA channel and f_s is the sampling rate. So the frequency estimation value of the received single-frequency signal is

$$\hat{f_n} = \arg\max_f \left|Y[z_k]\right|^2, 1 \leq n \leq 3. \tag{18}$$

We mark the estimation result as $\hat{f_1}, \hat{f_2}, \hat{f_3}$ and further acquire the corresponding estimated value of the common large scale Doppler factor:

$$\hat{a}^n = \frac{\hat{f_n} - f_n}{f_n}, 1 \leq n \leq 3. \tag{19}$$

Taking into account that there may be some inaccuracy at individual frequency points, we take the median of $\hat{a}^n$ as the estimated Doppler scaling factor $\hat{a}$.

As for compensation, we rely on a multiphase interpolation filter to resample the signal and get the resampled one: $y_m(n) = r(\frac{n}{1+\hat{a}})$,where the relation between input and output of sampling rate converter of L/M-times can be illustrated as Eq.20[11]:

$$y(n) = \sum_{i=0}^{K-1} h(\langle nM \rangle_L + iL) \cdot x(\left\lfloor \frac{nM}{L} \right\rfloor - i), \tag{20}$$

where $x[n]$is the signal to be resampled, $h(n)$ is the unit impulse response of a FIR (Finite Impulse Response) filter, whose length is N. It is divided into L subfilters, whose length is K. $\langle nM \rangle_L$ means a modular arithmetic to L and $\lfloor \frac{nM}{L} \rfloor$ denotes rounding down.

3.2 Residual Doppler Estimation and Compensation

Due to the deviation of large scale Doppler estimation and resampling, the OFDM system still suffers from the residual Doppler factor. Therefore, the residual Doppler factors $\beta_m = \frac{a-\hat{a}+a_m}{1+\hat{a}}$ need to be estimated and compensated for each OFDM symbol, respectively.

We suppose that the number of null subcarriers is K, the location information of null subcarriers is $K = [k_1, k_2, \cdots, k_K]$ and the m-th OFDM symbol after large scale Doppler compensation in Chapter 3.1 is $y_m(n)$. Assume that the preset residual estimation interval length is len,the interval left value is $\beta_{m,l}$,the right one is $\beta_{m,r}$. Then we can use the dichotomization to get our estimation value $\hat{\beta}_m$ for the m-th OFDM symbol:

Algorithm 1 Dichotomization

Initialization:
$\beta_{m,l} = PresetLeftValue, \beta_{m,r} = PresetRightValue$
$len = PresetRightValue - PresetLeftValue$
Iteration:
while $len > 1 \times 10^{-5}$ **do**
  $R_l(i) = \sum_{n=0}^{N-1} y_m(\frac{n}{1+\beta_{m,l}}) \times e^{-j2\pi \frac{ni}{N}}, i = [0 \quad N-1]$
  $Y_l(j) = R_l(k_j), j = 1, 2, \cdots, K$
  $J_l(j) = Y_l(j) \times Y(j)^H$
  $R_r(i) = \sum_{n=0}^{N-1} y_m(\frac{n}{1+\beta_{m,r}}) \times e^{-j2\pi \frac{ni}{N}}, i = [0 \quad N-1]$
  $Y_r(j) = R_r(k_j), j = 1, 2, \cdots, K$
  $J_r(j) = Y_r(j) \times Y(j)^H$
  if $J_l(j) < J_r(j)$ **then**
    $\beta_{m,r} = \frac{\beta_{m,l}+\beta_{m,r}}{2}$
  else
    $\beta_{m,l} = \frac{\beta_{m,l}+\beta_{m,r}}{2}$
  end if
  $len = len/2$
end while
$\hat{\beta}_m = \frac{\beta_{m,l}+\beta_{m,r}}{2}$

When the Doppler factor estimate is closer to the true value, the energy on the compensated null subcarrier is smaller. Like the algorithm above, to reduce the amount of computation, we use the method of bisection to determine residual Doppler factor within a pre-defined search range. Comparing the total energy of signal resampled by both ends of Doppler factor search range, we can determine which half of the search range is left. So the range will be halved again and again until the estimated interval is less than the predetermined value. Each OFDM symbol just requires 4-5 times of resampling and FFT to reach the goal that the residual Doppler search range is less than 1×10^{-5}. The amount of computation is much smaller than the method of traversal interval[5].

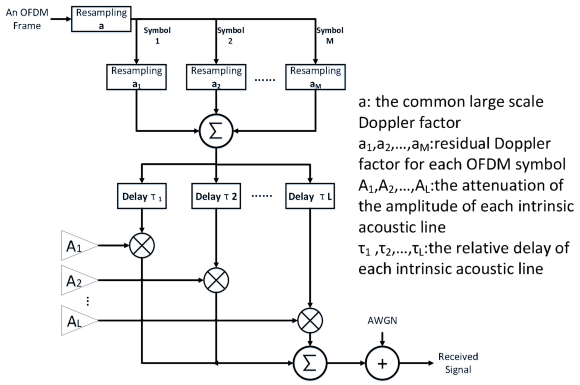

Figure 5: Channel Construction Method.

Hence, according to the obtained residual Doppler factor $\hat{\beta}_m$ for the m-th symbol, we resample the symbol $y_m(n)$ again with $1 + \hat{\beta}_m$ via resampling mentioned in 3.1 and get the resampled symbol $Z_m(n) = y_m(\frac{n}{1+\hat{\beta}_m})$, which achieves the Doppler compensation for the second time.

However, resampling can not eliminate the unequal phase rotation values caused by sampling timing offset due to residual Dopple. Therefore, it is necessary to correct the phase deviation described in Chapter 2. Knowing that $\phi_m[p,p] = \sum_{n=0}^{N-1} e^{j2\pi \frac{p}{N} \Delta N_m}$ is the value of phase rotation caused by residual Doppler, we can correct the corresponding phase in the frequency domain for each subcarrier of each symbol based on the calculated phase deflection value $C_m[p,p] = e^{-j2\pi \frac{p}{N} \Delta N_m}$, where $\Delta N_1 = 0$ and

$$\Delta N_m = \sum_{k=1}^{m-1} \frac{N_{cp} + N}{1 + \hat{\beta}_k}, m > 1. \tag{21}$$

4 SIMULATIONS AND EXPERIMENTS

4.1 Simulation Results Analysis

In order to verify the feasibility and validity of the proposed algorithm, we simulate it in baseband OFDM TD system like Fig.2 by MATLAB software. With regard to the construction of the channel, we use a multi-path Doppler channel as shown in Fig.5. The m-th OFDM symbol is affected by Doppler $(a + a_m)$ and then the signal passes through multi-path fading, multi-path delay-controlled channel with Gaussian white noise.

Fig.6 is the generated signal frame format. The LFM is a linear chirp signal with a frequency range of 6-12 kHz, followed by a serial and parallel single-frequency probe signal and an OFDM frame respectively. The frequencies of the three single-frequency signals are 6957.99 Hz, 8019.999 Hz and 9082.008 Hz. They are all integer

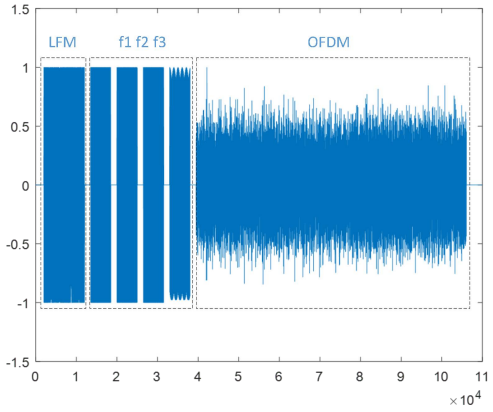

Figure 6: Signal frame format.

Table 1: Main parameters of OFDM system

Parameters	Values
sampling rate/kHz	50
frequency range/kHz	6 ~ 12
FFT length	4096
interval of subcarriers/Hz	12.207
encoding method	(2,1,3) convolutional encoding
mapping method	DQPSK
coding efficiency	0.5
duration of symbol/ms	81.9
duration of cyclic prefix/ms	20.5

multiples of the frequency resolution f_s/N. Each frame of OFDM signal contains 36 symbols. And We insert a null subcarrier before every three data subcarriers for the residual Doppler estimation. The arrangement of the null subcarriers is similar to comb pilot. Other main parameters are shown in Table 1.

Firstly, we have compared the performance of large scale Doppler estimation based on *FFT* and *CZT* in serial and parallel modes via root mean square error(RMSE) as shown in Fig.7.

$$RMSE = \sqrt{E\left[\sum(\hat{a}-a)^2\right]}. \tag{22}$$

We can see that: the *FFT* method has a higher error platform, which proves its infeasibility due to the fixed frequency resolution f_s/N. Due to the error of resampling and influence of estimation step size, there still exists a certain error platform(about 4×10^{-5}) for *CZT* method. It is lower than the *FFT* method and provides a narrower estimation range for residual Doppler estimation. The *CZT* method has a better performance than the *FFT* one. Besides, whether it is *CZT* or *FFT*, the performance of serial mode is similar to the parallel one at a high SNR. While at a SNR lower than 2dB, the performance of serial mode is better.

Secondly, generally the total energy left on null subcarriers after compensation show the performance of an algorithm, here we compare it with the increasement of residual Doppler after direct

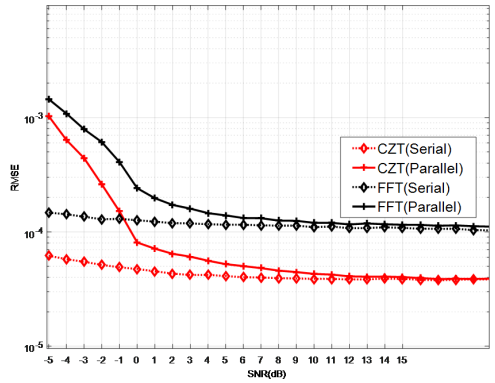

Figure 7: Performance Comparision of Frequency-domain Estimation Methods based on *FFT* and *CZT*.

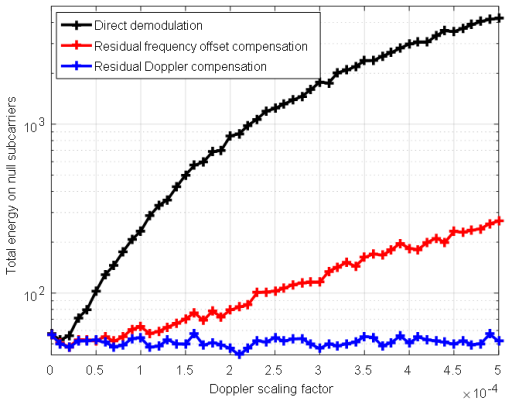

Figure 8: Sum of Energy on Null Subcarriers.

demodulation, residual frequency offset compensation[5] and residual Doppler compensation. The result is shown is Fig.8. Although both methods mitigate redidual Doppler effect, when residual Doppler factor is large($> 1\times10^{-4}$), residual Doppler is regarded as uniform frequency offset in residual frequency offset estimation, which makes its performance worse than the proposed residual Doppler estimation.

Furthermore, we analyze the influence of the phase rotation caused by the sampling timing offset via the TD demodulated constellation. In order to analyze the result intuitively, we set the channel to single path and noiseless. We suppose the common large scaling factor a has been eliminated. The residual Doppler factor is set as $a_m = 1\times10^{-4}$ and we can see the result in Fig.9 that *ICI* from residual Doppler can be effectively reduced after resampling in residual Doppler compensation, and the problem of residual Doppler phase rotation due to sampling timing offset can be effectively solved after phase compensation described in Chapter 3.2.

Finally, we analyze the effectiveness of the proposed algorithm and compare it with the classic *wideband to narrowband* approach[5][1] to estimate and compensate Doppler. Assume large-scale Doppler estimation has narrowed the Doppler scaling factor estimation range

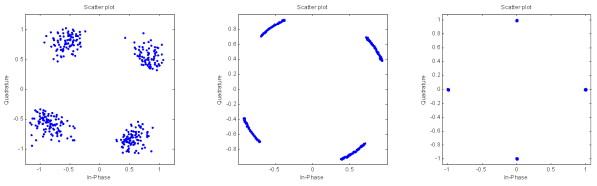

(a) After large-scale Doppler compensation (b) After residual Doppler resampling (c) After phase rotation compensation

Figure 9: Demodulated constellation

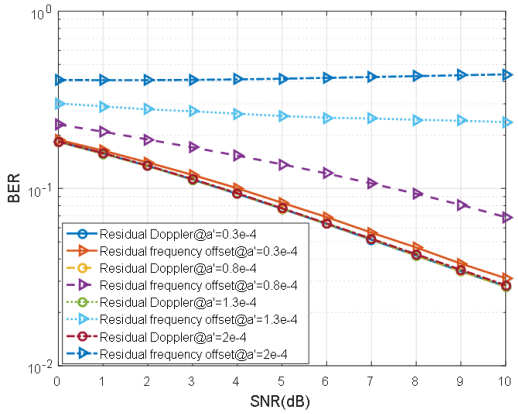

Figure 10: BER comparison between different methods.

to the level of $10^{-4} - 10^{-5}$, it can be seen from Fig.10 that when $a_m > 0.8 \times 10^{-4}$, residual frequency offset estimation can not perform well. And when $a_m > 1.3 \times 10^{-4}$, it fails to contribute to the mitigation of Doppler. In contrast, our residual Doppler estimation effectively mitigates the Doppler effect with all these residual Doppler scaling factors. Fig.11 shows the comparison among classical *wideband to narrowband* estimation and compensation(*E&C*), our algorithm and no Doppler process with $a = 5 \times 10^{-3}$ or $a = 0$. It can be verified that when the relative movement between the transmitting end and the receiver causes Doppler shift, the performance of the system hardly changes regardless of SNR[10]. After the Doppler mitigation of the proposed algorithm, the system performance is close to the situation of no Doppler effect. Combined with Fig.9 and Fig.11, we can draw the conclusion that the proposed algorithm effectively resolves the problem of phase rotation caused by sampling timing offset which was not solved in the classical *wideband to narrowband* algorithm[5] and thus reduces the bit error rate.

4.2 Experiment Results and Analysis

We conducted the experiments of relative uniform and nonuniform motion between the source and receiver in the pool. Experiment scheme I is shown in Fig.12. The transmitter and receiver were located at a depth of about 1 meters. The transmitter was fixed and the receiver moved towards and then away from the transmitter repeatedly, realizing the relative uniform movement between them. In experiment scheme II shown in Fig.13, the transmitter and receiver were located on two parallel rails, respectively. The

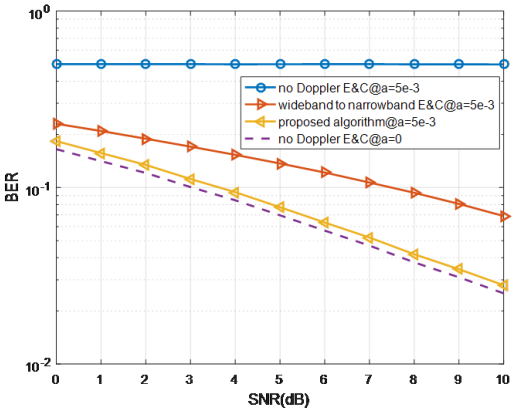

Figure 11: BER of the overall algorithm.

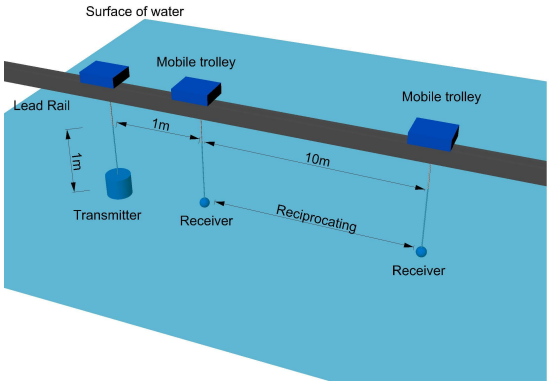

Figure 12: The configuration of relative uniform motion in pool.

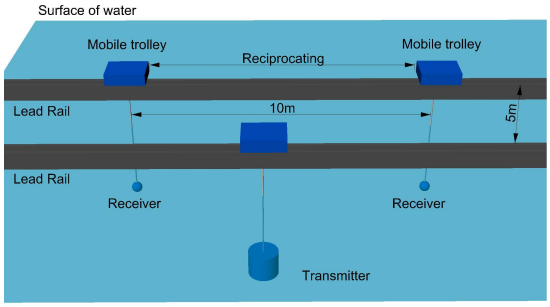

Figure 13: The configuration of relative nonuniform motion in pool.

transmitter was fixed and we moved the receiver making a relative nonuniform notion between them.

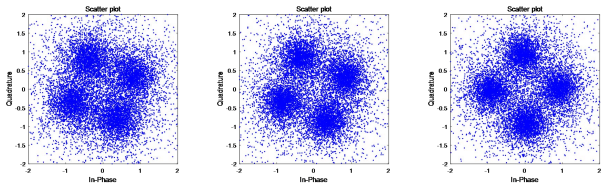

(a) After large-scale Doppler compensation (b) After residual Doppler resampling (c) After phase rotation compensation

Figure 14: Demodulated constellation

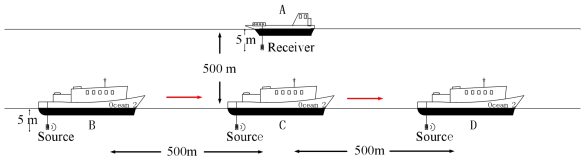

Figure 15: Sailing scheme.

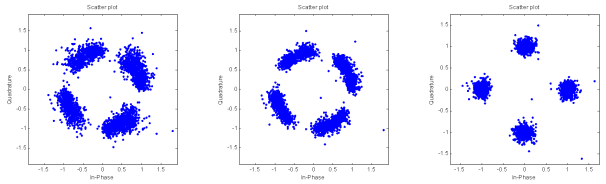

(a) After large-scale Doppler compensation (b) After residual Doppler resampling (c) After phase rotation compensation

Figure 16: Demodulated constellation

The transmitting transducer and receiving hydrophone were placed according to the scheme I and II, and the mobile trolley moved uniformly at a speed of $0.5m/s$. Fig.14 shows the constellations of differential demodulated signal after twice resampling compensation and phase rotation compensaton in the pool experiment. It can be seen that when the estimation is accurate enough, the impact of Doppler on the system can be mitigated after three times of compensation. Comparing Fig.14a, Fig.14b and Fig.14c, it can be seen that *ICI* can be mitigated after resampling in residual Doppler compensation, making the QPSK symbols more concentrated. And the phase rotation compensation described in Chapter 3.2 effectively overcomes the phase rotation caused by residual Doppler and enables the symbol to be correctly demodulated.

Further, we conducted the experiment again in Xiamen Bay following the scheme as Fig.15. The receiver was stationary and the transmitter made a straight line at 5 knots, bringing a time-varing Doppler scaling factor due to different angles between the moving direction and the connection of transmitter and receiver. Fig.16 shows the demodulated QPSK data constellation after twice resamplings and the phase rotation compensation. By comparing Fig.16a, Fig.16b and Fig.16c, we find again that residual Doppler resampling eliminates residual Doppler factor left by large-scale Doppler compensation and Doppler phase rotation compensation solves the problem of phase rotation. Through the sea trial, we further affirm the validity and practicability of the propose algorithm for eliminating the Doppler effect.

5 CONCLUSIONS

In this paper, we propose a Doppler estimation and compensation algorithm suitable for mobile underwater acoustic communication. In the large-scale Doppler estimation method, we use *CZT* to coarsely estimate the Doppler scaling factor. Due to a refinement of the spectrum, *CZT* method has a higher estimation resolution than the *FFT* method. It can also be used for real-time communication compared to the block-to-block time-domain estimation method[5]. In the residual Doppler estimation, null subcarriers are inserted, which ensures a higher estimation accuracy for each OFDM symbol. And then Doppler phase rotation compensation can effectively solve the problem of phase rotation introduced by sampling timing offset due to residual Doppler and further improve system performance.

Compared with the classical *wideband to narrowband* algorithm of Doppler removal[5][1], the proposed algorithm performs a higher accuracy of Doppler estimation and eliminates the phase rotation. And it can effectively overcome the disadvantages of lack of real-time operability in traditional Doppler time-domain estimation algorithms. In addition, we reduce the computational complexity significantly by the dichotomization. In other words, the proposed algorithm is designed to combine estimation accuracy with computational complexity.

6 ACKNOWLEDGMENTS

The work is supported by key laboratory open subject funding from Key Laboratory of Technology and Application For Safeguarding of Marine Rights and Interests, SOA (Grant No. 1708). Deqing Wang is also supported by the Research Fund for the Visiting Scholar Program by the China Scholarship Council (Grant No. 201506315026).

REFERENCES

[1] A. E. Abdelkareem, B. S. Sharif, C. C. Tsimenidis, J. A. Neasham, and O. R. Hinton. 2011. Low-complexity Doppler compensation for OFDM-based underwater acoustic communication systems. In *Oceans*. Santander, Spain, 1–6.
[2] J. P Costas. 1983. A study of a class of detection waveforms having nearly ideal range?Doppler ambiguity properties. *Proc. IEEE* 72, 8 (1983), 996–1009.
[3] R.C Heimiller. 1961. Phase shift pulse codes with good periodic correlation properties. *Information Theory Ire Transactions on* 7, 4 (1961), 254–257.
[4] Yong Hwa Kim and Jong Ho Lee. 2011. Comparison of Passband and Baseband Transmission Schemes for Power-Line Communication OFDM Systems. *IEEE Transactions on Power Delivery* 26, 4 (2011), 2466–2475.
[5] Baosheng Li, Shengli Zhou, Milica Stojanovic, Lee Freitag, and Peter Willett. 2008. Multicarrier Communication Over Underwater Acoustic Channels With Nonuniform Doppler Shifts. *IEEE Journal of Oceanic Engineering* 33, 2 (2008), 198–209.
[6] Qin Lu, Yi Huang, Zhaohui Wang, and Shengli Zhou. 2016. Characterization and receiver design for underwater acoustic channels with large Doppler spread. In *Oceans*. Washington,USA, 1–6.
[7] Xuefei Ma, Gang Qiao, and Zongxin Sun. 2013. A Method of Underwater Acoustic OFDM Adaptive Search Doppler Compensation.
[8] Nathan Parrish, Sumit Roy, and Payman Arabshahi. 2009. Symbol by symbol Doppler rate estimation for highly mobile underwater OFDM. In *WUWNet*. Berkeley, California, 1–8.
[9] L. I. Ping, Zhi Hui Zhao, and Zhen Ren Zhang. 2006. Effect of Sampling Clock Offsets on the Performance of OFDM System. *Information & Electronic Engineering* 4, 6 (2006).
[10] Zhanqing Pu, Wei Wang, Yangfan Zhang, Yu Li, and Haining Huang. 2017. Time-variant Doppler tracking and compensation in underwater acoustic OFDM communication for UUV platform. *Chinese Journal of Scientific Instrument* (2017).
[11] Yan Qiu and Yu Liu. 2009. Research and simulation of polyphase filter arithmetic in water acoustic signal processing. *Technical Acoustics* 28, 1 (2009), 82–84.
[12] F. Qu, Z. Wang, L. Yang, and Z. Wu. 2016. A journey toward modeling and resolving doppler in underwater acoustic communications. *IEEE Communications*

Magazine 54, 2 (2016), 49–55.

[13] L Rabiner, R. W Schafer, and C. M Rader. 1969. The chirp z-transform algorithm. *Audio & Electroacoustics IEEE Transactions on* 17, 2 (1969), 86–92.

[14] B. S Sharif, J Neasham, O. R Hinton, and A. E Adams. 2000. A computationally efficient Doppler compensation system for underwater acoustic communications. *IEEE Journal of Oceanic Engineering* 25, 1 (2000), 52–61.

[15] M Stojanovic. 2006. Low Complexity OFDM Detector for Underwater Acoustic Channels. In *Oceans*. 1–6.

[16] Milica Stojanovic and James Preisig. 2009. Underwater acoustic communication channels: Propagation models and statistical characterization. *IEEE Communications Magazine* 47, 1 (2009), 84–89.

[17] H. Susaki. 2002. Method of high-resolution frequency measurement for pulse-Doppler sonar. In *International Symposium on Underwater Technology*. 39–44.

[18] Lei Wan, Zhaohui Wang, Shengli Zhou, T. C. Yang, and Zhijie Shi. 2012. Performance comparison of doppler scale estimation methods for underwater acoustic OFDM. *Journal of Electrical and Computer Engineering,2012,(2012-5-30)* 2012, 2090-0147 (2012), 1.